International Journal of Fluid Power 9 (2008) No. 1 pp. 35-43

OPTIMAL MODE SWITCHING FOR A HYDRAULIC ACTUATOR CONTROLLED WITH FOUR-VALVE INDEPENDENT METERING CONFIGURATION

Amir Shenouda and Wayne Book

Georgia Institute of Technology, Woodruff School of Mechanical Engineering, 801 Ferst Dr. NW, Atlanta, GA, 30332, USA
amir.shenouda@gatech.edu, wayne.book@me.gatech.edu

Abstract

A spool valve is a single degree of freedom system that has coupled 'meter in' and 'meter out'. Decoupling of meter in from meter out provides for more controllability and potential for energy saving in overrunning load cases when compared with a conventional spool valve controlled hydraulic system. A four-valve configuration controlling a hydraulic cylinder is emphasized in this paper. The four-valve configuration can operate in several two-valve discrete modes because each of the four valves is controlled separately from the others. Five distinct (or discrete) metering modes that exist in the literature are initially studied: Powered Extension, High Side Regeneration Extension, Low Side Regeneration Extension, Powered Retraction, and Low Side Regeneration retraction. Each of these modes has different force and speed capabilities and the operating mode should consequently be selected based on the load and the commanded speed. Proper switching between these modes is crucial for efficient and productive performance.

The problem of switching between these five modes is treated as an optimal control problem of a switched dynamic system. General theory for the optimal control problem is derived and then applied to the hydraulic system of interest. The results are then interpreted and explained by looking into the force-speed capability of modes, and a closed form solution for the quasi static case is presented.

Keywords: hydraulics, independent metering valves, metering modes, mode capability curve, mode switching

1 Introduction

The idea of using a four-valve assembly to achieve independent metering control of hydraulic actuators has been discussed in previous work by several researchers including Jansson (1990); Tabor (2004, 2005); Yao (2002); and Shenouda and Book (2005, 2006), for example. Figure 1 shows the four valve independent metering configuration. Four valves are needed to operate one cylinder. These valves are usually poppet type valves. The valves used in this research are two stage poppet valves. One valve connects one of the work ports of the cylinder to the supply line that contains pressurized oil. A second valve connects the other work port to the supply line. A third valve connects the first port to return line which leads to the tank. Finally a fourth valve is needed to connect the second port to the return line. Using this four valve configuration, while only two valves will be active for a given condition, allows for independent metering and also allows for energy regeneration as explained in Stephenson (2003); Tabor (2004); and Kramer (1996), which has the potential of reducing the requirements on the pump and thus achieve highly valuable energy saving. The four-valve configuration can operate in several modes because each of the four valves is controlled separately from the others. These modes are presented in the following section.

This manuscript was received on 28 June 2007 and was accepted after revision for publication on 31 January 2008

2 Two-Valve Discrete Metering Modes

Figure 1 is a schematic that shows the concept of using a four-valve configuration to achieve independent metering. There are five distinct metering modes that describe the operation of a hydraulic cylinder controlled by a four-valve assembly as shown in Fig. 1. This configuration is investigated by Tabor and Pfaff (2004, 2005).

2.1 Powered Extension (PE) Mode

The operation of this mode is not necessarily different from the operation of a cylinder controlled by a conventional proportional directional control spool valve. Flow is supplied at high pressure from the pump through valve K_{sa} into head chamber A of the cylinder causing the piston to move (extend). This piston motion forces the flow out of rod chamber B through valve K_{bt} to the tank. The difference, however, is that in this four-valve configuration K_{sa} and K_{bt} can be controlled separately, while in a conventional proportional valve they cannot be controlled independently as explained in the introduction.

2.2 Powered Retraction (PR) Mode

In this case, flow is supplied at high pressure from the pump through valve K_{sb} into rod chamber B of the cylinder causing the piston to move (retract). This piston motion forces the flow out of head chamber A through valve K_{at} to the tank.

2.3 High Side Regeneration Extension (HSRE) Mode

This is one of the regenerative modes that can be achieved by the four-valve configuration and could not be achieved by a conventional proportional directional control valve. Flow coming out of rod chamber B at high pressure does not go to tank through valve K_{bt}, but it circulates through valves K_{sb} and K_{sa} into head chamber A causing the piston to move (extend). However, the flow coming out of chamber B is less than the flow needed in chamber A to achieve a certain speed because of the difference in areas ($A_a > A_b$). Flow out of either chamber is $Q = A \cdot V$ and for a given velocity and with the difference in area ($Q_a > Q_b$). The remaining flow is supplied from the pump, but it is just enough to make up of the difference in flow while in powered extension mode all the flow is supplied from the pump. Thus, the High Side Regeneration Extension mode has the potential to save energy if the load is below a certain value. This is discussed later in section 5.

2.4 Low Side Regeneration Extension (LSRE) Mode

Flow coming out of rod chamber B does not go to tank but it circulates through valve K_{bt} and K_{at} into head chamber A causing the piston to move (extend). However, the flow coming out of chamber B is less than the flow needed in chamber A to achieve a particular speed as explained above. The remaining flow can be supplied from the pump, but it is just enough to make up of the difference in flow and it is supplied at a low pressure.

2.5 Low Side Regeneration Retraction (LSRR) Mode

Flow coming out of head chamber A does not go to tank but it circulates through valve K_{at} and K_{bt} into rod chamber B causing the piston to move (retract). The flow coming out of chamber A is more than the flow needed in chamber B to achieve some speed as explained above. The extra flow goes to tank through the check valve. Thus, no pump flow at all is needed for this mode, which means a high potential for saving energy whenever this mode is used.

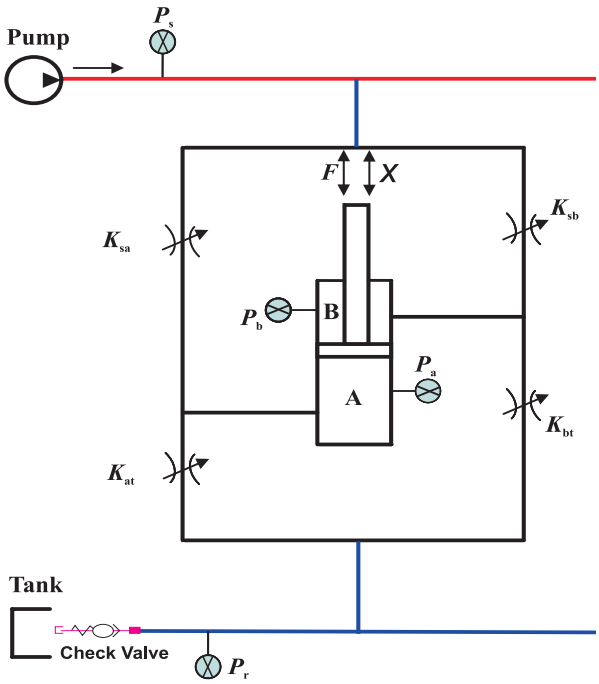

Fig. 1: *Four valve independent metering configuration*

3 Valve Control for Discrete Modes

Valve control for the configuration shown in Fig. 1 has been derived and presented by Tabor (2004, 2005). An overview of this valve control methodology is presented in this section. The word discrete in the title of this section refers to the different modes referred to above but does not mean that the valves are discrete on/off valves. The individual valves are proportional, i.e. variation in current commanded to these valves corresponds to variation in the opening size of the valves and that is used for velocity (flow) control. The conductance or opening size of the valves are represented by a variable parameter K followed by a subscript to clarify which valve in the circuit it represents. The analysis conducted in this paper does not take into consideration the hydraulic line losses. Details are shown in the references by Tabor and Pfaff (2004, 2005). Tabor and Pfaff applied a quasi static analysis assuming that the plant dynamics are much slower than the controller and ignored capacitance effects. Figure 2 shows a cylinder in Powered Extension mode. Tabor (2005) showed that this system is mathematically equal to an equivalent pressure source P_{eq}, and equivalent valve conductance K_{eq} as shown in the figure. The equivalent pressure and equivalent conductance can be expressed by:

$$P_{eq} = R(P_s - P_a) + (P_b - P_r)$$
$$K_{eq} = \frac{K_{sa} K_{bt}}{\sqrt{K_{sa}^{\,2} + R^3 K_{bt}^{\,2}}} \qquad (1)$$

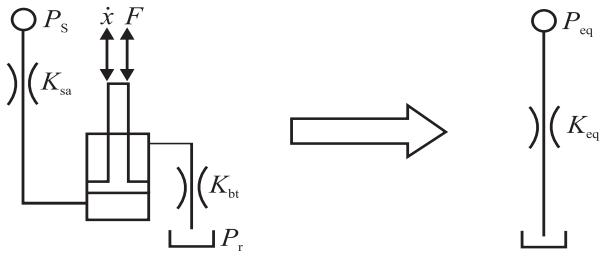

Fig. 2: *Mathematically equivalent systems: valve control overview (Tabor, 2005)*

where R is the area ratio between the two piston sides $R = \frac{A_a}{A_b}$. Tabor (2005) showed that there are infinitely many combinations of K_{sa} and K_{bt} values that would achieve the same K_{eq} value. A certain K_{eq} corresponds to a certain actuator speed given a certain load, supply, and return pressures by Eq. 2:

$$\dot{x} = \frac{K_{eq}\sqrt{P_{eq}}}{A_b} = \frac{K_{eq}\sqrt{\left(RP_s - P_r\right) + \left(-RP_a + P_b\right)}}{A_b} \tag{2}$$

For High Side Regeneration Extension mode the equation turns out to be:

$$\dot{x} = \frac{K_{eq}\sqrt{P_{eq}}}{A_b} = \frac{K_{eq}\sqrt{\left(R-1\right)P_s + \left(-RP_a + P_b\right)}}{A_b} \tag{3}$$

Similar equations can be derived for the other modes (Tabor, 2004, 2005).

4 Optimal Mode Switching

This section looks at the problem of switching between two modes as a problem of optimal switching of a switched dynamic system. General theory is first developed for this problem and then the results are applied to the mode switching problem of the hydraulic system under investigation in this paper. What complicates this mode switching problem is that not only the dynamics of the system changes upon mode switching, but the cost function of the optimal control problem changes as well.

4.1 Switched Dynamic Systems

A switched dynamic system is such that its dynamic behavior can be described by a finite number of dynamic models, in the form of differential equations, and a set of rules that controls switching between these different dynamic models. These dynamic models describe discrete system behaviors with different characteristics.

The hydraulic system in this research can be portrayed as a switched dynamic system that has different dynamic behaviors based upon which metering mode it is operating in. For example, an actuator can start motion in PE mode then switches to HSRE mode, which has different dynamic behavior than PE with different force and speed capabilities.

The following mathematical expression is often used to describe switched dynamical systems:

$$\dot{x}(t) \in \left\{ f_\sigma\left(x(t), u(t)\right)\right\}_{\sigma \in A} \tag{4}$$

where $x(t) \in R^n$, $u(t) \in R^k$ and $\left\{ f_\sigma\left(x(t), u(t)\right)\right\}_{\sigma \in A}$ is a group of continuously differentiable functions parameterized by σ which $x(t) \in R^n$, $u(t) \in R^k$ a set A (Egerstedt, et al., 2003). Time t is between 0 and T. Many applications in chemical, automotive, and manufacturing systems can be modeled by such switched systems representation (Xu and Antsaklis, 2004).

Optimal control of these switched dynamical systems, which requires finding the optimal switching time between different continuous systems and at the same time the optimal continuous inputs has been under research recently (Xu and Antsaklis, 2004, Branicky, M. S., et al., 1998) because of its importance in several applications. Control analysis and stability of such systems to achieve autonomous and intelligent control are under intense research activities. The reference mentioned here and the references therein are a good example of recent developments in the literature.

The work here, however, focuses on a class of autonomous systems where $u(t)$ is absent from the problem formulation because it is predetermined, and the variable to be controlled optimally is the switching time (Xu and Antsaklis, 2002).

In Xu and Antsaklis (2002), an optimization problem is setup in terms of a cost function of the state to be minimized with the control variable being the switching times. The results are then used for nonlinear programming algorithms. This reference provides a starting point for later work. However, a simpler cost function gradient formula is derived here.

This optimal control problem where the cost function is the same throughout the time interval under consideration but the dynamics of the system change after a certain switching time has been considered and a simple solution has been found (Egerstedt, et al., 2003). In the problem considered in this research, the cost function itself changes after switching happens, not just the dynamics of the system. If the hydraulic system switches from PE to HSRE, the dynamics of the system change and also the pressure and flow characteristics change. If the cost function is a function of pressure and flow, then the cost function itself changes upon mode switching. This is going to be explained further in the problem formulation section.

4.1.1 Problem Formulation

Assume that a system behaves according to certain dynamics $\dot{x} = f_1(x,t)$ and then at time $\tau \in [0,T]$ the system dynamics change to $\dot{x} = f_2(x,t)$. This can be expressed by the following:

$$\dot{x} = \begin{cases} f_1(x,t) & t \in [0,\tau) \\ f_2(x,t) & t \in [\tau,T] \end{cases} \tag{5}$$

Now consider a continuously differentiable function $L: \ ^n \rightarrow$ and the cost functional J where:

$$J = \int_0^T L\left(x(t)\right) dt \tag{6}$$

In this problem we consider the control variable to be the switching time τ. If $L(x(t))$ is the same through out the time interval $[0,T]$, the solution to this optimal problem already exists in the literature (Egerstedt, et al., 2003). The gradient of J is found to be:

$$\frac{dJ}{d\tau} = \lambda(\tau)\left(f_1\left(x(\tau)\right) - f_2\left(x(\tau)\right)\right) \tag{7}$$

Where the costate λ (Lagrange multiplier-like variable) equation is given by:

$$\begin{aligned} \dot{\lambda} &= -\frac{\partial L}{\partial x} - \lambda \frac{\partial f_2}{\partial x} \\ \lambda(T) &= 0 \end{aligned} \tag{8}$$

In this work, however, the function $L(x(t))$ is not the same through out the time interval $[0,T]$. If $L(x(t))$ represents the power consumption which depends on the flow and supply pressure from the pump, and since each mode has different flow and supply pressure requirement, $L(x(t))$ will change upon mode switching. The cost function can be expressed as:

$$J = \int_0^{\tau} L_1\left(x(t)\right)\, dt + \int_{\tau}^{T} L_2\left(x(t)\right)\, dt \tag{9}$$

Thus, not only the dynamics of the system change when switching happens, but the cost function changes as well.

4.1.2 Gradient Calculation

In this section the gradient of the cost function J in Eq. 9 is calculated. Since τ is the control variable in this problem, consider a perturbation in $\tau : \tau \to \tau + \varepsilon\theta$ where ε >> 1. This perturbation in τ results in a change in the state $x \to x + \varepsilon\eta$. This is shown in Fig. 3.

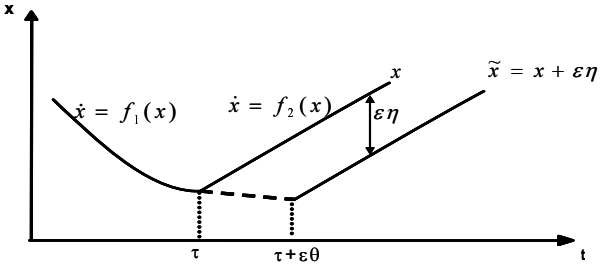

Fig. 3: *Switching and perturbation*

The cost function of the τ perturbed system is:

$$\begin{aligned} J(\tau+\varepsilon\theta) = &\int_0^{\tau}\left[L_1\left(x(t)\right) + \lambda\left(f_1\left(x(t)\right) - \dot{x}(t)\right)\right]dt + \\ &\int_{\tau}^{\tau+\varepsilon\theta}\left[L_1\left(x+\varepsilon\eta\right) + \lambda\left(f_1\left(x+\varepsilon\eta\right) - \dot{x} - \varepsilon\dot{\eta}\right)\right]dt + \\ &\int_{\tau+\varepsilon\theta}^{\tau}\left[L_2\left(x+\varepsilon\eta\right) + \lambda\left(f_2\left(x+\varepsilon\eta\right) - \dot{x} - \varepsilon\dot{\eta}\right)\right]dt \end{aligned} \tag{10}$$

$$\begin{aligned} &\frac{J(\tau+\varepsilon\theta) - J(\tau)}{\varepsilon} = \\ &\int_{\tau}^{\tau+\varepsilon\theta}\left[L_1 + \frac{\partial L_1}{\partial x}\eta + \lambda\left(f_1 + \frac{\partial f_1}{\partial x}\eta - f_2 - \varepsilon\dot{\eta}\right) - L_2\right]dt + \\ &\int_{\tau+\varepsilon\theta}^{T}\left[\frac{\partial L_2}{\partial x}\eta + \lambda\left(\frac{\partial f_2}{\partial x}\eta - \varepsilon\dot{\eta}\right)\right]dt \end{aligned} \tag{11}$$

Using the mean value theorem:

$$\begin{aligned} &\int_{\tau}^{\tau+\varepsilon\theta}\left[L_1 - L_2 + \lambda(t)\left(f_1 - f_2\right)\right]dt = \\ &\varepsilon\theta\left[L_1\left(x(\tau)\right) - L_2\left(x(\tau)\right) + \lambda(\tau)\left(f_1\left(x(\tau)\right) - f_2\left(x(\tau)\right)\right)\right] \end{aligned} \tag{12}$$

In the interval $\tau : \tau \to \tau + \varepsilon\theta$ the terms multiplied by $\varepsilon\eta$ are small higher order terms that can be ignored.

Using integration by parts:

$$\int_{\tau}^{T}\lambda\dot{\eta}\,dt = \lambda(T)\eta(T) - \lambda(0)\eta(0) - \int_{\tau}^{T}\dot{\lambda}\eta\,dt \tag{13}$$

Note that $\eta(0) = 0$.

Obtaining the Gateaux derivative by taking the limit of the expression in Eq. 11 with respect to ε and combining with Eq. 12 and 13:

$$\begin{aligned} &\delta J(\tau,\theta) = \lim_{\varepsilon\to 0}\frac{J(\tau+\varepsilon\theta) - J(\tau)}{\varepsilon} = \\ &\left[L_1\left(x(\tau)\right) - L_2\left(x(\tau)\right) + \lambda(\tau)\left(f_1\left(x(\tau)\right) - f_2\left(x(\tau)\right)\right)\right] + \\ &\int_{\tau}^{T}\left(\frac{\partial L_2}{\partial x} + \lambda\frac{\partial f_2}{\partial x} + \dot{\lambda}\right)\eta\,dt + \lambda(T)\eta(T) \end{aligned} \tag{14}$$

Choosing λ (a Lagrange multiplier-like variable called costate) such that:

$$\begin{aligned} \dot{\lambda} &= -\frac{\partial L_2}{\partial x} - \lambda\frac{\partial f_2}{\partial x} \quad on\ t \in [\tau, T] \\ \lambda(T) &= 0 \end{aligned} \tag{15}$$

the gradient is found to be:

$$\begin{aligned} \frac{dJ}{d\tau} &= L_1\left(x(\tau)\right) - L_2\left(x(\tau)\right) + \\ &\lambda(\tau)\left(f_1\left(x(\tau)\right) - f_2\left(x(\tau)\right)\right) \end{aligned} \tag{16}$$

The optimal solution is obtained when the gradient in Eq. 16 is zero, but in practical applications several numerical techniques can be used to obtain the optimal switching time, τ_{opt}. For example, a simple gradient descent algorithm can be used as indicated by the following equation.

$$\tau_{k+1} = \tau_k - \gamma\frac{dJ}{d\tau} \tag{17}$$

The algorithm tries to minimize the difference between τ_{k+1} and τ_k until that difference is below a certain threshold.

5 Force-Speed Mode Capability Curve

In this section the force-speed capability curves of Powered Extension (PE) and High Side Regeneration Extension (HSRE) modes are presented. A quasi-static assumption is made here as well, and hydraulic line losses are neglected in the analysis. The speed that the actuator can achieve is limited by how much flow the pump can supply. The force capability that the actuator can provide depends on the load itself and the maximum supply pressure that the pump can supply.

5.1 PE Force-Speed Capability

The speed of the actuator can be expressed in terms of hydraulic force for PE mode by making use of Eq. 2 as follows:

$$F = P_a A_a - P_b A_b \tag{18}$$

$$\dot{x}_{PE} = \frac{K_{eq}\sqrt{RP_s - \frac{F}{A_b} - P_r}}{A_b} \tag{19}$$

The required power is used to quantify the force limitation due to supply pressure constraint and velocity limitation due to pump maximum flow restriction:

$$\begin{aligned} &Power = P \cdot Q = F \cdot \dot{x} \\ &P \cdot Q_{PE} = F_{max} \cdot \dot{x}_{PE} = (P_s A_a - P_r A_b)\dot{x}_{PE} \\ &\Rightarrow Q_{PE} = \frac{(P_s A_a - P_r A_b)\dot{x}_{PE}}{P_s} \end{aligned} \tag{20}$$

If Q_{PE} is calculated to be more than Q_{max}, then the speed $\dot{x}_{PE}$ is limited so that $Q_{PE} = Q_{max}$. Using Eq. 20:

$$\dot{x}_{PE} = \frac{Q_{max} P_s}{(P_s A_a - P_r A_b)} \tag{21}$$

5.2 HSRE Force-Speed Capability

A similar analysis can be done for HSRE mode. The speed of the actuator can be expressed in terms of the hydraulic force for HSRE mode using Eq. 3 as follows (Tabor, 2004):

$$\dot{x}_{HSRE} = \frac{K_{eq}\sqrt{(R-1)P_s - \frac{F}{A_b}}}{A_b} \tag{22}$$

The required power is used to quantify the force limitation due to supply pressure constraint and velocity limitation due to pump maximum flow restriction:

$$\begin{aligned} &Power = P \cdot Q = F \cdot \dot{x} \\ &P_s Q_{HSRE} = F_{max} \cdot \dot{x}_{PE} = P_s (A_a - A_b)\dot{x}_{HSRE} \\ &\Rightarrow Q_{HSRE} = (A_a - A_b)\dot{x}_{HSRE} \end{aligned} \tag{23}$$

If Q_{HSRE} is calculated to be more than Q_{max}, then the speed $\dot{x}_{HSRE}$ is limited so that $Q_{HSRE} = Q_{max}$. Using Eq. 23:

$$\dot{x}_{HSRE} = \frac{Q_{max}}{(A_a - A_b)} \tag{24}$$

An actual telehandler machine extender cylinder is used as an example. Assuming maximum valve opening, a force range from 0 → 100 KN is used to plot the force-speed curve for PE and HSRE modes as shown in Fig. 4. The maximum pump flow is 5520 L/h. Figure 4 shows both mode capability curves superimposed on each other. The figure shows that PE mode has a higher force capability of about 97 KN (in this example) than HSRE, which can push a maximum load of about 50.3 KN. However, HSRE has a maximum speed capability of about 0.8 m/s while PE has a maximum speed capability of 0.4 m/s.

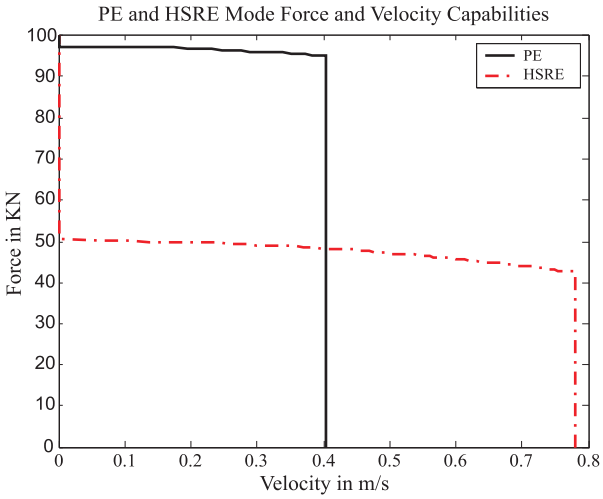

Fig. 4: *PE and HSRE mode force-speed capability curves*

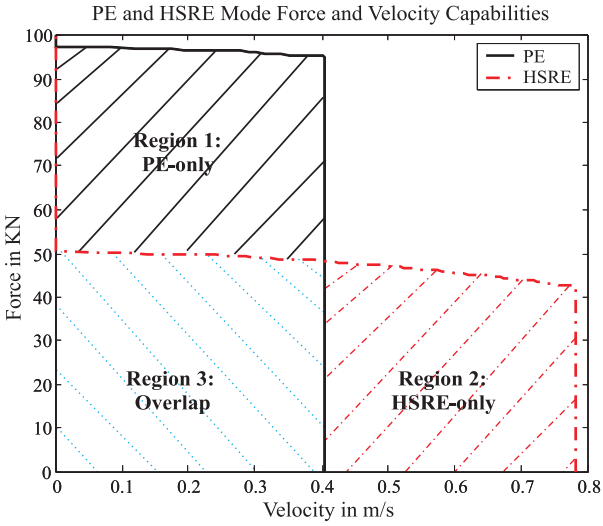

Fig. 5: *Three regions of capability*

Coordination between using these two modes and optimally switching between them is essential to achieving high machine productivity and efficiency. This is the topic for the following section.

Figure 5 shows that there are three different regions. Region 1 is the PE-only region which represents a region where only PE mode is able to move the load, while the Region 2 is the HSRE-only region, and finally the third is an overlap region where both modes can achieve the motion commanded.

In regions one and two, it is obvious which mode has to be used, while in region three it is not obvious which one is to be used. Applying the optimal switching theory developed in section 4 to the hydraulic system helps to decide which mode is to be used as discussed next.

6 Application of Optimal Mode Switching to the Hydraulic System

The result derived in section 4.1.2 Gradient Calculation is now applied to a hydraulic actuator controlled by the four-valve independent metering configuration. Focus is on a system that is assumed to start in Powered Extension mode for high force capability at the beginning of motion and then switches into High Side Regeneration mode to achieve the maximum speed possible.

The cost function is chosen to be the energy consumed by the machine in a fixed time *T*. *L* in this case is the power consumption:

$$J = \int_0^T L\left(x(t)\right)\,\mathrm{dt} = \int_0^T P_s.Q_s\,\mathrm{dt} \tag{25}$$

where P_s is the supply pressure and Q_s is the supply flow. Therefore, L_1 would be the power consumption in PE mode, while L_2 would be the power consumption in HSRE mode. Flow is expressed as follows:

$$Q_s = Q_{sa} - Q_{sb} = K_{sa}\sqrt{P_s - P_a} - K_{sb}\sqrt{P_b - P_s} \tag{26}$$

For PE mode, $K_{sb} = 0$ and $Q_s = Q_{sa}$, while for HSRE K_{sb} is open and there is a flow Q_{sb}. Supply pressure required depends on the mode as well. Pressure set point equation for both PE and HSRE are (Tabor, 2005):

$$P_{s,PE} = \frac{P_{eq,min}}{R} + \frac{\left(RP_a - P_b\right)}{R} + \frac{P_r}{R} \tag{27}$$

$$P_{s,HSRE} = \frac{P_{eq,min}}{R-1} + \frac{\left(RP_a - P_b\right)}{R-1} \tag{28}$$

Where $P_{eq,min}$ is the minimum pressure needed to maintain a certain pressure drop across the poppet valves for good dynamic response.

For the quasi-static case the gradient in Eq. 16 is reduced to the difference between the power consumed by both modes at the switching point because f_1 and f_2 are equal in the quasi static case:

$$\frac{dJ}{d\tau} = L_1\left(x(\tau)\right) - L_2\left(x(\tau)\right) \tag{29}$$

$$\Rightarrow \frac{dJ}{d\tau} = P_{S,PE}Q_{S,PE} - P_{S,HSRE}Q_{S,HSRE} \tag{30}$$

The optimal solution is achieved when:

$$\frac{dJ}{d\tau} = 0 \tag{31}$$

Equation 30 shows that for the gradient to be zero the power consumption has to be the same and that is achieved at the intersection point in Fig. 4 where the power consumption is equal in both modes. The optimal switching point is shown in Fig. 6.

$$\Rightarrow P_{S,PE}Q_{S,PE} = P_{S,HSRE}Q_{S,HSRE} \tag{32}$$

Power can also be expressed as force times speed and thus Eq. 32 is equivalent to the following:

$$\begin{aligned} Power_{\ PE} &= Power_{\ HSRE} \\ F_{PE}\dot{x}_{PE} &= F_{HSRE}\dot{x}_{HSRE} \end{aligned} \tag{33}$$

Where:

$$F_{PE} = P_s A_a - P_r A_b \tag{34}$$

$$\dot{x}_{PE} = \frac{K_{eq}}{A_b}\sqrt{RP_s - P_r - \frac{F}{A_b}} \tag{35}$$

$$F_{HSRE} = P_s\left(A_a - A_b\right) \tag{36}$$

$$\dot{x}_{HSRE} = \frac{K_{eq}}{A_b}\sqrt{\left(R-1\right)P_s - \frac{F}{A_b}} \tag{37}$$

Substituting in Eq. 28:

$$\begin{aligned} &\left(P_s A_a - P_r A_b\right)\frac{K_{eq}}{A_b}\sqrt{RP_s - P_r - \frac{F}{A_b}} = \\ &P_s\left(A_a - A_b\right)\frac{K_{eq}}{A_b}\sqrt{\left(R-1\right)P_s - \frac{F}{A_b}} \end{aligned} \tag{38}$$

Assuming that $P_r \approx 0$, Eq. 38 can be solved for *F*, the load at which optimal switching should occur:

$$F = P_s A_b \frac{3R^2 - 3R + 1}{2R - 1} \tag{39}$$

Substituting *F* from Eq. 39 into Eq. 35 or 37, the corresponding optimal switching speed is obtained

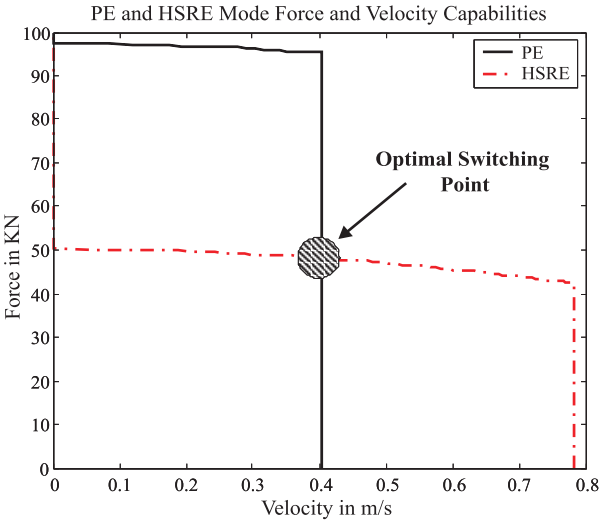

Fig. 6: *Optimal switching point*

Given a certain maximum supply pressure, maximum flow, cylinder sizes, the force and speed calculated from the quasi static analysis above will always be the intersection point shown above in Fig. 6.

For an efficient and proper motion path, this result implies motion starts in PE mode and should continue in PE mode until load is within the capability of HSRE mode, then switching should occur. To illustrate this on

the mode capability curve, refer to Fig. 6. An example motion path would be to start at zero speed with high force in the PE-only possible region, then traversing horizontally as speed increases with some downward tendency as load decreases due to lowered inertia effects. This path continues until the maximum speed limit of PE mode is reached and the path becomes vertical downward along that boundary. This continues until the optimal switching point is reached and switching to HSRE occurs and the motion path can start to go horizontal again allowing more speed. This is illustrated in Fig. 7.

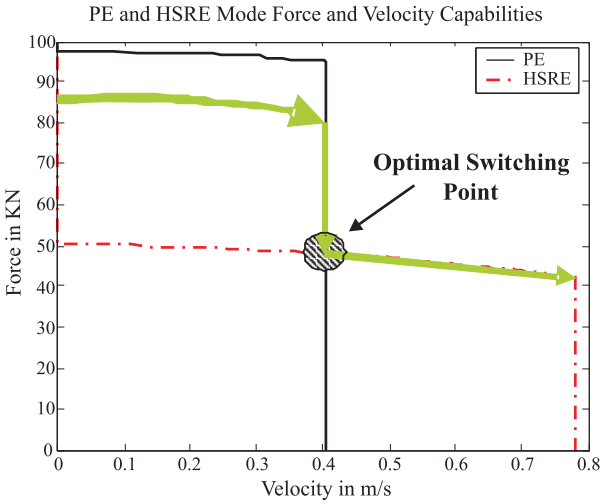

Fig. 7: *Example mode switching scenario*

6.1 Results

An experiment is done to quantify the effect of changing switching time on telehandler productivity and efficiency. Productivity is measured by how long it takes to complete the full stroke of the extender and efficiency is measured by how much energy it consumes. The boom is put in a horizontal position and the extender is retracted fully before giving it a maximum speed command and data is recorded throughout the full stroke. Since the boom of the machine is horizontal, the load is within the capability of both PE and HSRE modes. In this experiment, controlling mode switching is done by cylinder position. First the full stroke is done in PE. Then the stroke is repeated with transition into High Side Regeneration Extension mode happening after three quarters of the stroke is performed in PE, then with transition happening at half stroke, then at quarter the stroke, and finally the whole stroke is performed in High Side Regeneration Extension mode. Table 1 shows the results. The results show that comparing full stroke in Powered Extension mode and full stroke in High Side Regeneration Extension mode, an energy saving of 30.7 % is achieved but with a 37.6 % loss in productivity (time to perform the stroke). The tradeoff is clear from the results in the table. The theoretical development tried to balance productivity and efficiency but if the goal is to achieve maximum productivity or maximum efficiency, the controller strategy will be different. For example, if the goal is strictly efficiency then the whole stroke will have to be entirely performed in PE mode.

6.2 Multiple Actuator Case

The situation can be different in a multiple actuator case. Assume that two actuators are being commanded at the same time. If each actuator is treated separately, the optimal switching point is the intersection point between PE and HSRE mode capability curves pertinent to the specific actuator. However, if this is applied without further insight, a waste of energy could occur. Assume that one actuator has to move a large load and thus demands a high pressure from the pump. The other actuator may be moving a smaller load but because the pump is already supplying a high pressure to the former actuator, it would save pump flow and thus pump power for the latter actuator to be operating in High Side Regeneration mode (HSRE) than Powered Extension mode (PE). As a consequence of this insight, the optimal switching point is no longer that intersection point but the second actuator should switch to HSRE right away.

To explain this further, suppose that the second actuator is operating in the overlap region in Fig. 5, i.e. the region where both PE and HSRE can move the load at the required speed. The results from previous section indicate that optimally the actuator should operate in PE until the intersection point or the maximum PE velocity boundary is reached then switch to HSRE mode. However, since pressure is up already and operation in HSRE is feasible, the second actuator should switch to HSRE and continue motion in HSRE to save flow.

Conclusions

The four-valve independent metering configuration controlling a hydraulic cylinder is investigated in this paper. The four-valve configuration can operate in several two-valve discrete modes because each of the four valves is controlled separately from the others. Five distinct (or discrete) metering modes that exist in the literature are initially studied: Powered Extension, High Side Regeneration Extension, Low Side Regeneration Extension, Powered Retraction, and Low Side Regeneration Retraction. Each of these modes has different force and speed capabilities and the operating mode should consequently be selected based on the load and the commanded speed, and switching properly between these modes is crucial for good performance.

Table 1: Variation of energy consumption and stroke time with switching point

Switching Point	Time to Complete Stroke (sec)	Enery Consumed (kJ)
All Stroke in PE	6.6	46.2
Switching at 3/4 Stroke	5.9	49.8
Switching at 1/2 Stroke	5.6	57.7
Switching at 1/2 Stroke	4.7	65.1
All Stroke in HSRE	4.1	66.7

Optimal control of mode switching was the focus of this paper. Switching between two discrete modes was studied as a problem of optimal switching of a switched dynamic system. The general theory was developed and then the dynamic model of the hydraulic system was used to apply the theoretical results to the mode switching problem. An example of switching between PE and HSRE mode was used for illustration. It was shown that for an efficient and a proper motion path, motion should start in PE mode and should continue in PE mode until load is within the capability of HSRE mode then switching should occur. The result showed that the optimal switching point is the intersection point shown on the mode capability curve. A closed form solution was derived for the quasi static case.

It is also clear from Fig. 4 that there are limitations to what the machine can do. For example, if the actuator needs to push a force of 50.3 KN, which is the maximum possible force using HSRE mode, at a commanded speed of 0.7 m/s it cannot. To push such a load, the actuator would have to operate in PE mode at a lower speed than what is commanded. Then, as motion progresses and inertia effects decrease, i.e. load decreases, switching to HSRE mode may become possible and achieving the commanded speed becomes possible as well.

The multiple actuator case discuss in this paper indicates that the theory should not be applied at all times. The controller will have to discern opportunities to optimize the performance of the system. Also, the result presented in the paper assumes equal importance between efficiency and productivity. That may not always be the case. In some cases productivity could be more important than efficiency and vice versa. Again, the system controller should have the versatility to change priorities depending on the application.

In addition to mode capability limitations, switching between PE and HSRE during motion can have an effect on velocity performance. Switching between modes involves closing one poppet valve and opening another. These valves are not infinitely fast and thus an interruption in the fluid flow path resulting from mode switching causes a disruption in the velocity of the actuator.

Other metering modes may exist that increase the capacity envelopes (force speed limitation) of these modes and alleviate the velocity disruption problem. These alternative modes depend on three-valve modulation modes instead of the two-valve discrete modes presented in this paper. These alternative modes are the topic for another paper.

Acknowledgements

This work is partially supported by HUSCO International. The cooperation of the engineering development team at HUSCO International is greatly appreciated.

Nomenclature

P_{eq}	equivalent pressure	[Mpa]
P_s	supply pressure	[MPa]
P_r	return pressure	[MPa]
P_a	head chamber workport pressure	[MPa]
P_b	rod chamber workport pressure	[MPa]
q_a	flow through head chamber (a)	[m^3/sec]
q_b	flow through rod chamber (b)	[m^3/sec]
K	valve conductance	[m^3/sec/ $(MPa)^{0.5}$]
K_{eq}	equivalent valve conductance	[m^3/sec/ $(MPa)^{0.5}$]
R	piston area ratio	[-]
A_a, A_b	piston head and rod areas	[mm²]

References

Branicky, M. S., **Borkar, V. S.**, and **Mitter, S. K.** 1998. A Unified framework for hybrid control: Model and optimal control theory. *IEEE Transactions on Automatic Control*, vol. 43, pp. 31-45, January.

Egerstedt, M., **Wardi, Y.** and **Delmott, F.** 2003. Optimal control of switching times in switched dynamical systems. *IEEE Conference on Decision and Control*, Maui, Hawaii, December.

Jansson, A. and **Palmberg, J-O.** 1990. Separate control of meter in and meter out orifices in a mobile hydraulic systems. *SAE Technical Paper* (901583).

Kramer, K. D. and **Fletcher, E. H.** 1996. *Electrohydraulic valve system*. United States Patent (Re,33,846).

Liu, S. and **Yao, B.** 2002. Energy saving control of single-rod hydraulic cylinders with programmable valve sand iporved working model selection. *National Fluid Power Association*, Vol. 102, no. 24, pp. 81-91.

Pfaff, J. and **Tabor, K.** 2004. *Method of sharing flow of fluid among multiple hydraulic functions in a velocity based control system*. United States Patent (6,779,340).

Pfaff, J. and **Tabor, K.** 2004. *Velocity based electronic control system for operating hydraulic equipment*. United States Patent (6,732,512).

Shenouda, A. and **Book, W.** 2005. Energy savings analysis using a four valve independent metering configuration controlling a hydraulic cylinder. *SAE Commercial Vehicle Engineering Conference*, Chicago, Illinois.

Shenouda, A. and **Book, W.** 2005. Selection of operating modes of a multi-functional hydraulic device. *IMECE Conference*, Orlando, Florida.

Shenouda, A. 2006. *Quasi-Static Hydraulic Control Systems and Energy Savings Potential Using Independent Metering Four-Valve Assembly Configuration*. PhD Dissertation, Georgia Institute of Technology, Atlanta, Georgia.

Stephenson, D. B. 2003. *Hydraulic system with cross function regeneration*. United States Patent (5,502,393).

Tabor, K. 2004. *Velocity based method for controlling a hydraulic system*. United States Patent (6,718759).

Tabor, K. 2004. *Velocity based method for controlling an electro-hydraulic proportional control valve*. United States Patent (6,775,974).

Tabor, K. 2005. A novel method of controlling a hydraulic actuator with four valve independent metering using force feedback. *SAE Commercial Vehicle Engineering Conference*, Chicago, Illinois.

Tabor, K. 2005. Optimal velocity control and cavitation prevention of a hydraulic actuator using four valve independent metering. *SAE Commercial Vehicle Engineering Conference*, Chicago, Illinois.

Xu, X. and **Antsaklis, P.** 2002. Optimal control of switched autonomous systems. *IEEE Conference on Decision and Control*, pp. 2063-2068.

Xu, X. and **Antsaklis, P.** 2004. Optimal control of switched dynamical systems based on parameterization of switching instants. *IEEE Transactions on Automatic Control*, vol. 49, pp. 2-16.

Amir Shenouda
Amir Shenouda received his Bachelor of Science in Mechanical engineering from The American University in Cairo in 1999. He received his Master of Science in Mechanical Engineering from Gannon University in 2002. He obtained a Masters of Science in Electrical Engineering and a Ph.D. in Mechanical Engineering from the Georgia Institute of Technology in 2006. His research focused on hydraulic control systems and specifically the four-valve independent metering configuration. Industrial experience includes Mercedes Benz, Bristol Myers, General Electric, HUSCO International, and Parker Hannifin.

Wayne Book
Wayne J. Book received his B.S.M.E. degree from the University of Texas at Austin in 1969 and the M.S. and Ph.D. degrees in mechanical engineering from the Massachusetts Institute of Technology in 1971 and 1974, respectively. Wayne Book has been on the faculty of Mechanical Engineering at the Georgia Institute of Technology since 1974 where he is a Professor and the HUSCO/Ramirez Distinguished Professor in Fluid Power and Motion Control. His research includes the design, dynamics and control of high speed, lightweight motion systems, robotics, fluid power and motion control and haptics. He is a Fellow of the ASME, SME, and IEEE, and received Georgia Tech's award for Outstanding Faculty Leadership for development of Graduate Research Assistants in 1987, and an ASME Dedicated Service Award in 2003 and the ASME DSCD Leadership Award in 2004.